Available online at www.sciencedirect.com
SCIENCE DIRECT®

Journal of the European Ceramic Society 23 (2003) 2403–2408
www.elsevier.com/locate/jeurceramsoc

Structure and microwave dielectric properties of $La(Mg_{0.5}Ti_{0.5})O_3$–$CaTiO_3$ system

M.P. Seabra[a], M. Avdeev[a], V.M. Ferreira[a], R.C. Pullar[b], N.McN. Alford[b]

[a]*Department of Ceramic and Glass Engineering/CICECO, University of Aveiro, 3810-193 Aveiro, Portugal*
[b]*Centre for Physical Electronics and Materials, Faculty of Engineering, Science and Technology, South Bank University, 103 Borough Road, London SE1 0AA, UK*

Abstract

$(1-x)La(Mg_{0.5}Ti_{0.5})O_3$ (LMT)–$xCaTiO_3$ (CT) $[0<x<1]$ ceramics were prepared from powder obtained by a nonconventional chemical route based on the Pechini method. The crystal structure of the microwave dielectric ceramics has been refined by Rietveld method using X-ray powder diffraction data. LMT and CT were found to form a solid solution over the whole compositional range. The 0.9LMT–0.1CT composition was refined using $P2_1/n$ space group, which allows taking into account B-site ordering. The compounds having $x \geqslant 0.3$ were found to be disordered and were refined using Pbnm space group. Microstructure evolution was also analysed. Dielectric characterization at microwave frequencies was performed on the LMT–CT ceramics. The permittivity and the temperature coefficient of resonant frequency of the solid solutions showed a non-linear variation with composition. The quality factor demonstrates a considerable decrease with the increase of CT content.

Keywords: Powders–chemical preparation; X-ray methods; Dielectric properties; Perovskites; $La(Mg,Ti)O_3$; $CaTiO_3$

1. Introduction

The revolution that occurred in the last decade in wireless communications and information access stimulated an interest in dielectric materials, which are used as the basis for resonators and filters for microwave applications. These applications require a combination of high dielectric permittivity (ε), near-zero temperature coefficient of resonant frequency (τ_f) and high quality factor (Q). A higher permittivity value enables the resonator size to be reduced. A very small temperature coefficient of resonant frequency (less than ± 10 ppm/°C) is necessary for the stability of the device at room temperature. The quality factor of dielectric resonators determines their frequency selectivity. These requirements are almost always mutually exclusive in dielectric materials.

Recently, a number of complex perovskites with the general formula $A(B'_{1/2}B''_{1/2})O_3$ have been reported as having moderate permittivities (20–35) combined with negative τ_f (<-26 ppm/°C) and high quality factors ($Q \cdot f > 30{,}000$ GHz),[1–7] which made them candidate materials for microwave dielectrics. The value of τ_f of such materials can be shifted to zero by preparation of solid solutions with compounds having positive temperature coefficient of resonant frequency.[5,6] Factors affecting the microwave dielectric properties can be divided into two groups: intrinsic, related with the characteristics of the lattice (order-disorder phenomena and anharmonicity of lattice vibrations) and extrinsic, mainly related with processing (density, phase inhomogeneity, etc.).[8]

There have been some attempts to correlate the structural characteristics of perovskite compounds with their dielectric properties.[5,6,9–12] It was demonstrated that B-site cation ordering in complex perovskites $A^{3+}B^{3+}O_3$ and $A^{2+}B^{4+}O_3$, such as $Ba(Zn_{1/3}Ta_{2/3})O_3$,[9] $(1-x)La(Zn_{1/2}Ti_{1/2})O_3$–$xSrTiO_3$[6] and $Ba(Ni_{1/3}Nb_{2/3})O_3$,[10] is very important for achieving high quality factors. The significance of the factors affecting τ_f like tilting of oxygen octahedra, cation ordering and short-range lattice modulation has also been reported.[5,11,12] Correlation between τ_f and octahedra tilting has been established by the example of $(Sr,Ba)(Zn_{1/3}Nb_{2/3})O_3$ system.[11] According to Colla et al.[11] the tilting of oxygen octahedra in perovskite compounds induces negative τ_f values due to an increase in lattice anharmonicity. On the other hand, a short-range modulation of crystal structure rather than a change in long-range crystal structure was suggested

E-mail addresses: pseabra@cv.ua.pt (M.P. Seabra); pseabra@cv.ua.pt (V.M. Ferreria).

0955-2219/03/$ - see front matter © 2003 Elsevier Ltd. All rights reserved.
doi:10.1016/S0955-2219(03)00142-0

as the origin of τ_f and ε anomalies in the $(Sr,Ba)(Zn_{1/3}Nb_{2/3})O_3$ system.[12] It was also suggested[5] in the system $La(Zn_{1/2}Ti_{1/2})O_3$–$ATiO_3$ (A = Ca, Sr), that cation ordering induces a negative τ_f and can suppress the increase of ε. However, the relation between octahedral tilting and τ_f does not apply to CT since this compound has octahedral tilting but its τ_f is positive.

As it has been reported, $La(Mg_{0.5}Ti_{0.5})O_3$ (LMT) is a promising microwave material having $\varepsilon = 27.4$–29, Q·f = 63,100–75500 GHz and $\tau_f = -65$–(−74) ppm/°C.[1,3,4,13] Structurally, LMT is a distorted B-site ordered perovskite (space group $P2_1/n$).[14] In contrast, $CaTiO_3$ (CT) has no cation ordering and exhibits high permittivity (145) and very positive τ_f (+712 ppm/°C).[15] A previous study of (1−x)LMT-xCT system was focused on three compositions in a narrow range of CT content ($x = 0.47$, 0.54 and 0.62).[16] As a part of current systematic study of microwave complex perovskites,[14,17] the objective of this study is further investigating of the structure and dielectric property relationships in a wide range of LMT–CT solid solution system.

2. Experimental procedure

(1−x)LMT–xCT ceramics ($x = 0.1$, 0.3, 0.5, 0.7 and 0.9) were prepared using powders obtained by a chemical route based on the Pechini method, optimised previously for LMT.[13] In this procedure, the precursor resin was calcined at 750 °C for 3 h in order to obtain the powders with the required compositions. The powder was isostatically pressed at 200 MPa and sintered at 1350–1600 °C over 2 h in air with heating and cooling rates 10 °C/min. For the samples with high CT contents ($x = 0.7$, 0.9) samples were also sintered in oxygen with the same sintering conditions in order to check atmosphere effect on microstructure and dielectric properties.

The sintered pellets were ground in order to obtain powders for X-ray diffraction (XRD) experiments. X-ray powder diffraction data were collected at room temperature using Rigaku D/MAX-B diffractometer (Bragg–Brentano geometry, CuK_α radiation, graphite monochromator, $2\theta = 15$–115, step 0.02, 7 s/step). Rietveld refinement was performed using GSAS suite.[18] When refining the occupancies of Mg and Ti sites, the unit cell content was constrained according to the nominal chemical composition.

Relative density of sintered samples was determined from geometry and weight measurements and their microstructure was examined by scanning electron microscopy (SEM) (Hitachi S-4100). The samples for SEM observations were polished and thermally etched 50 °C below the sintering temperature for 2 min. Chemical homogeneity of the samples was analysed by energy dispersive spectroscopy (EDS). Measurements of dielectric properties at microwave frequencies were performed by the Hakki–Coleman method[19] at room temperature. τ_f was obtained by measuring the variation in resonant frequency (f_r) in an oxygen-free high-conductivity copper cavity, between 230 and 300 K, while cooling at a rate of 2 °C min^{-1} (CTI Cryogenics Model 22 refrigerator and 8200 cryocompressor with a Lakeshore 330 Temperature Controller).[20]

3. Results and discussion

Fig. 1 shows the XRD patterns of the (1−x)LMT–xCT samples for different x values. The refinement results are summarized in Table 1. The refined atomic parameters are presented in Tables 2 to 6. No reflections of impurity phases were observed and therefore the formation of solid solutions in all the range can be concluded. The shift in 2θ values observed in this figure is due to the smaller lattice parameters of $CaTiO_3$. The extra reflections were indexed on the basis of the $\sqrt{2}a_p \times \sqrt{2}a_p \times 2a_p$ cell, where a_p is the lattice parameter of cubic perovskite. The relation between the appearance of the peaks with particular (hkl) indices and

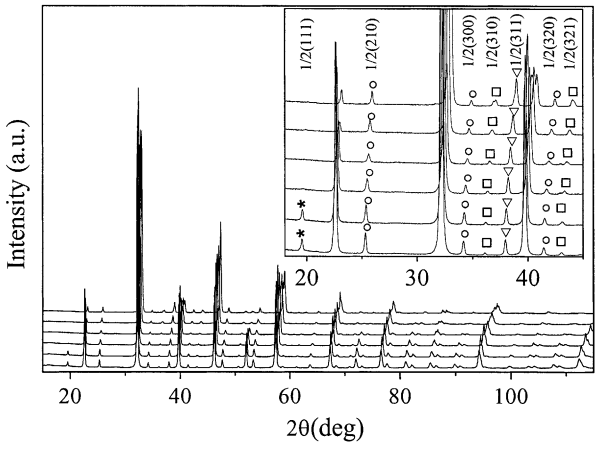

Fig. 1. XRD pattern of (1−x)LMT−xCT, $x = 0$ (bottom),[14] 0.1, 0.3, 0.5, 0.7, 0.9 (top). Inset shows supercell reflections indicating Mg/Ti ordering (stars), antiparallel La(Ca) displacement (circles), in-phase octahedra tilting (squares), anti-phase octahedra tilting (triangles).

Table 1
Summary of Rietveld refinement of (1−x)LMT−xCT ceramics[a]

X	Space group	R_p	R_{wp}	χ^2
0.1	**$P2_1/n$**	**6.51**	**4.67**	**4.865**
0.3	$P2_1/n$	5.06	6.64	5.435
	Pbnm	**4.81**	**6.45**	**5.216**
0.5	$P2_1/n$	5.94	7.57	5.186
	Pbnm	**5.75**	**7.34**	**5.011**
0.7	**Pbnm**	**4.63**	**5.56**	**3.340**
0.6	**Pbnm**	**5.35**	**6.46**	**3.847**

[a] The bold font indicates the finally chosen space group.

Table 2
Fractional atomic coordinates, thermal parameters and occupancies of 0.9LMT–0.1CT[a]

Atom	X	y	z	U*100, Å^2	Occupancy
La	0.49347(19)	0.52762(8)	0.2498(9)	0.720(15)	0.9
Ca	0.49347(19)	0.52762(8)	0.2498(9)	0.720(15)	0.1
Ti(1)	0.5(–)	0(–)	0(–)	0.40(22)	0.62
Mg(1)	0.5(–)	0(–)	0(–)	0.40(22)	0.38
Mg(2)	0(–)	0.5(–)	0(–)	0.32(23)	0.52
Ti(2)	0(–)	0.5(–)	0(–)	0.32(23)	0.48
O(1)	0.2869(28)	0.2541(23)	0.0453(27)	0.169(–)	1
O(2)	0.233(4)	0.8196(27)	0.0375(20)	0.169(–)	1
O(3)	0.5632(23)	0.9892(8)	0.237(4)	0.169(–)	1

[a] Cell parameters: $a = 5.55064(14)$ Å, $b = 5.56066(10)$ Å, $c = 7.84884(19)$ Å, $\beta = 90.003(20)^\circ$.

Table 3
Fractional atomic coordinates, thermal parameters and occupancies of 0.7LMT–0.3CT[a]

Atom	x	y	z	U*100, Å^2	Occupancy
La	−0.00418(33)	0.02505(9)	0.25(–)	1.091(2)	0.7
Ca	−0.00418(33)	0.02505(9)	0.25(–)	1.091(2)	0.3
Ti	0.5(–)	0(–)	0(–)	0.779(27)	0.65
Mg	0.5(–)	0(–)	0(–)	0.779(27)	0.35
O(1)	0.0650(15)	0.4880(7)	0.25(–)	1.00(8)	1
O(2)	−0.2765(10)	0.2820(9)	0.0398(8)	1.00(8)	1

[a] Cell parameters: $a = 5.52251(14)$ Å, $b = 5.53864(14)$ Å, $c = 7.81451(17)$ Å.

Table 4
Fractional atomic coordinates, thermal parameters and occupancies of 0.5LMT–0.5CT[a]

Atom	x	y	z	U*100, Å^2	Occupancy
La	−0.0035(4)	0.02466(11)	0.25(–)	1.079(1)	0.5
Ca	−0.0035(4)	0.02466(11)	0.25(–)	1.079(1)	0.5
Ti	0.5(–)	0(–)	0(–)	0.575(27)	0.75
Mg	0.5(–)	0(–)	0(–)	0.575(27)	0.25
O(1)	0.0616(14)	0.4895(7)	0.25(–)	0.59(7)	1
O(2)	−0.2781(9)	0.2805(8)	0.0387(7)	0.59(7)	1

[a] Cell parameters: $a = 5.49063(16)$ Å, $b = 5.51551(16)$ Å, $c = 7.77460(21)$ Å.

Table 5
Fractional atomic coordinates, thermal parameters and occupancies of 0.3LMT–0.7CT[a]

Atom	x	y	z	U*100, Å^2	Occupancy
La	−0.00617(27)	0.02705(10)	0.25(–)	1.618(20)	0.3
Ca	−0.00617(27)	0.02705(10)	0.25(–)	1.618(20)	0.7
Ti	0.5(–)	0(–)	0(–)	1.480(25)	0.85
Mg	0.5(–)	0(–)	0(–)	1.480(25)	0.15
O(1)	0.0720(10)	0.4820(6)	0.25(–)	2.48(6)	1
O(2)	−0.2860(27)	0.2850(6)	0.0343(5)	2.48(6)	1

[a] Cell parameters: $a = 5.45517(7)$ Å, $b = 5.48981(6)$ Å, $c = 7.72955(12)$ Å.

Table 6
Fractional atomic coordinates, thermal parameters and occupancies of 0.1LMT–0.9CT[a]

Atom	x	y	z	U*100, Å^2	Occupancy
La	−0.00662(27)	0.03099(12)	0.25(–)	1.940(25)	0.1
Ca	−0.00662(27)	0.03099(12)	0.25(–)	1.940(25)	0.9
Ti	0.5(–)	0(–)	0(–)	1.487(24)	0.95
Mg	0.5(–)	0(–)	0(–)	1.487(24)	0.05
O(1)	0.0731(7)	0.4843(5)	0.25(–)	2.56(5)	1
O(2)	−0.2870(4)	0.2881(4)	0.0358(4)	2.56(5)	1

[a] Cell parameters: $a = 5.40865(6)$ Å, $b = 5.46007(5)$ Å, $c = 7.67519(9)$ Å.

structural features like octahedral tilting, ordering, antiparallel displacement is explained elsewhere.[14,17]

In the 0.9LMT–0.1CT sample Mg and Ti cations are still partially ordered [supercell reflection 1/2(111)], like it was shown to exist in undoped LMT.[14] Therefore, the same space group $P2_1/n$ was used for the structure refinement. However, it should be noted that the degree of order decreases when increasing the CT content. The same behaviour was observed in other systems[14,17] with the addition of alkaline earth titanates.

The XRD patterns of the samples with $x = 0.3$ and 0.5 demonstrate no evidence of Mg/Ti chemical ordering and the refinement quality is higher when using Pbnm space group (which presupposes complete B-site disorder) instead of $P2_1/n$ (Table 1). The B-site ordering in complex perovskites is normally very dependent on composition, being very sensitive to slight deviations.[21] However, a similar behaviour of LMT–CT was observed in other systems ($La(Zn_{0.5}Ti_{0.5})$–$SrTiO_3$, $La(Zn_{0.5}Ti_{0.5})$–CT, LMT–$BaTiO_3$, LMT–$SrTiO_3$).[5,14,17]

The compositions with $x = 0.7$ and 0.9 also present an orthorhombic structure. The variation of the cell para-

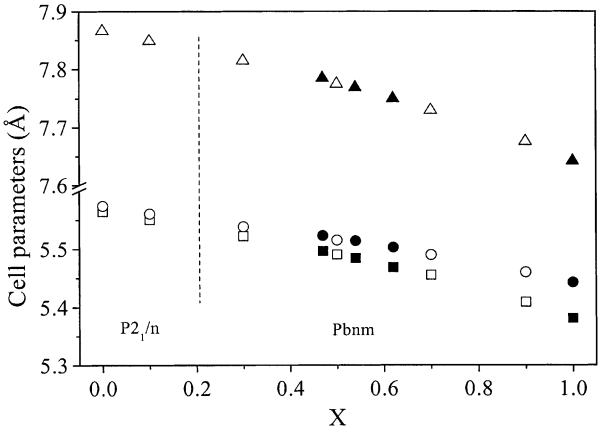

Fig. 2. Cell parameters as function of $CaTiO_3$ content (a—squares, b—circles, c—triangles). Filled symbols,[16] empty—this work, $CaTiO_3$ from JCPDS-ICDD card No. 22-153. The vertical dashed line is presented only to guide and do not represent an exact compositional phase transition.

meters with respect to the amount of CT shows a linear decrease with the increase of CT content (Fig. 2). The parameters were found to be in very good agreement with those reported[16] for three other compositions of LMT–CT system. The cell volume gradually decreases with x according to the substitution of La^{3+} and Mg^{2+} by the smaller Ca^{2+} and Ti^{4+} respectively.

The densification of $(1-x)$LMT–xCT samples was attained by sintering them between 1350 and 1600 °C in air and in oxygen for 2 h depending on the composition (see Table 7). The samples with high amounts of CT showed a different colour depending on the sintering atmosphere. For 0.7 and 0.9 of CT the samples sintered in air presented a darker colour than the ones sintered in oxygen and, for the same sintering conditions, a lower density value.

Polished and thermally etched surface of the sintered samples are shown in Fig. 3. The ceramics grain size varies with the concentration of $CaTiO_3$ and presents a uniform distribution in all cases. For $x=0$, 0.1, 0.3 and 0.5 the sintering conditions were the same and a remarkable increase of the grain size was observed, even for low CT contents ($x=0.1$). A pronounced difference in the microstructure is also observed for the samples sintered in air and oxygen. The samples with $x=0.7$ and 0.9 sintered in oxygen presents a smaller grain size and higher density values (Fig. 3 and Table 7).

Table 7 also presents microwave dielectric data on $(1-x)$LMT–xCT ceramics, where it is possible to observe that, regarding the end members, well optimized LMT samples presents a better Q value than the one previously reported[1,3,4,13] while the CT values were extracted from recent literature.[15]

Fig. 4 shows porosity corrected dielectric permittivity values of the $(1-x)$LMT–xCT ceramic system. With the increase in x values, the permittivity increases from 29.8 to 165.3. Although the samples were not mixtures of pure LMT and CT phases, the measured results were compared with calculated ones obtained from the empirical relationship for dielectric mixtures[22]: $\varepsilon^n = \Sigma \nu_i \varepsilon_i^n$, where ν_i and ε_i are the volume fraction and permittivity of each phase i, respectively. Using this rule it was found that, for $n=-1$, the relation described well the measured permittivities (Fig. 4). This means that permittivity of these samples can be regarded as a frac-

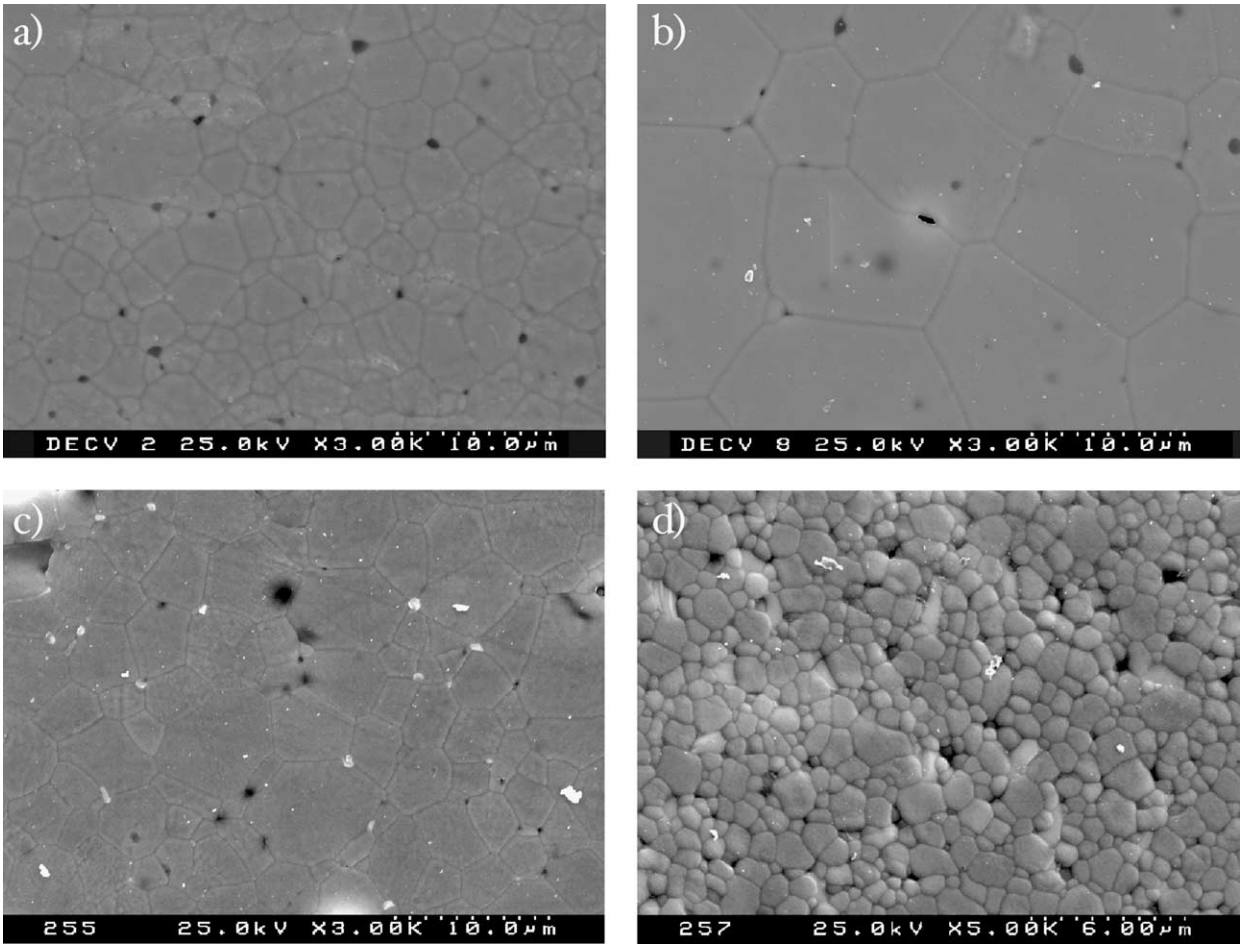

Fig. 3. SEM photographs of $(1-x)$LMT–xCT sintered (during 2 h) specimens thermally etched polished surface; (a) $x=0.1$; (b) $x=0.5$ sintered at 1600 °C in air; $x=0.7$ sintered at 1500 °C on (c) air and (d) O_2.

Table 7
Dielectric properties in the (1–x)LMT–xCT system

x	Sintering conditions	Density (%)	ε	ε_c[a]	τ_f	Q	f_r (GHz)	Qf (GHz)
0	Air/1600 °C	97.0	27.6	29.4	−81	16110	7.10	114312
0.1	Air/1600 °C	95.3	29.8	32.6	−70	2438	6.86	16725
0.3	Air/1600 °C	99.1	37.2	38.2	−54	2426	6.32	15322
0.5	Air/1600 °C	95.7	43.2	46.7	−13	2263	5.50	12437
0.7	Air/1500 °C	88.5	51.2	62.4	–	7587	5.78	43884
	O_2/1500 °C	95.8	58.8	63.3	+71	7266	5.56	40395
0.9	Air/1350 °C	88.8	90.4	109.1	–	7048	4.54	31963
	O_2/1350 °C	94.7	102.5	111.9	+395	4720	4.28	20180
1[b]	Air	92.0	145	163.3	+712	800	2.20	1760

[a] Corrected for porosity.[25]
[b] Data from.[15]

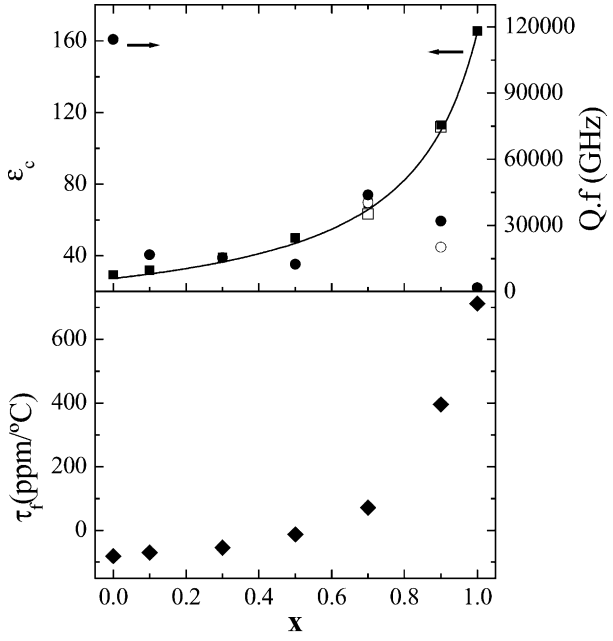

Fig. 4. Microwave dielectric properties of (1−x)LMT−xCT (dotted line indicates the calculated values based on the mixture rule). For $x=0.7$ and 0.9 (ε and Q.f) the open symbols are values for the samples sintered in O_2. Values for CT were taken from the literature.[15]

tional sum of the permittivity of the end members as it was observed for other perovskite systems which involve $A(B'_{1/2}B''_{1/2})O_3$ and either $CaTiO_3$ or $SrTiO_3$.[5,6,15,23,24]

In Fig. 4, τ_f of LMT–CT samples also showed a non-linear variation with no singularity, analogous to ε variation for the same samples. Similar behaviour was observed in other systems [$La(Zn_{0.5}Ti_{0.5})$–$SrTiO_3$, $La(Zn_{0.5}Ti_{0.5})$–CT].[5,6]

The quality factor of the samples is expressed in terms of the Q.f product. As can be seen in Fig. 4, Q.f of the samples shows a sharp decrease for $x=0.1$ and then remains approximately constant. According to some authors,[6,9,10] Q can be related with the cation ordering, causing its absence often a decrease on Q. Although it is still present for $x=0.1$, the degree of cation ordering is less than in the undoped LMT, and this could be one of the reasons for the decrease on Q. It should be noted that Levin et al.[15] suggested that Q might also reflect the influence of other factors besides the ones related with crystal structure. For high CT contents ($x=0.7$ and 0.9) the samples sintered in O_2, although presenting a higher density showed Q.f values dose to the ones sintered in air. It should be noted that for the same sintering time the grain is also smaller for O_2 sintered samples.

4. Conclusions

Single-phase, dense ceramics of compositions (1−x)LMT–xCT ($0<x<1$) were prepared from powders obtained by a chemical route. A wide range solution was confirmed in this system.

For $x=0.1$ the system still has some Mg/Ti ordering being the XRD data successfully refined using the $P2_1/n$ space group as for LMT. For higher CT contents the B-site ordering disappeared and Pbnm space group was assigned. The cell volume gradually decreases with x.

The microstructure is homogeneous for all the compositions and the grain size increase with the increase of CT content. No second phases were detected. Regarding the microwave dielectric properties ε follows a typical mixture rule as in a two phase composite system. τ_f also showed a nonlinear variation with composition. The presence of CT strongly affected the Q value which showed a sharp decrease for $x=0.1$ and then remained approximately constant. The sintering atmosphere (air or O_2) affects densification, microstructure and dielectric properties of the samples with high CT contents ($x=0.7$ and 0.9).

Acknowledgements

M.P. Seabra and V.M. Ferreira wish to acknowledge the support of the Foundation for Science and Technology (FCT), Portugal.

References

1. Cho, S. Y., Kim, C. H., Kim, D. W., Hong, K. S. and Kim, J. H., Dielectric properties of $Ln(Mg_{1/2}Ti_{1/2})O_3$ as substrates for high-T_c superconductor thin films. *J. Mater. Res.*, 1999, **14**(6), 248–2487.
2. Cho, S. Y., Seo, M. K., Hong, K. S., Park, S. J. and Kim, I. T., Influence of ZnO evaporation on the microwave dielectric properties of $La(Zn_{1/2}Ti_{1/2})O_3$. *Mater. Res. Bull.*, 1997, **32**(6), 725–735.
3. Cho, S. Y., Ko, K. H., Hong, K. S. and Park, S. J., Cation ordering and microwave dielectric properties of complex perovskite compounds $La(Mg_{1/2}Ti_{1/2})O_3$ and $La(Mg_{1/2}Zr_{1/2})O_3$. *J. Korean Ceram. Soc.*, 1997, **34**(3), 330–336.
4. Lee, D. Y., Yoon, S. J., Yeo, J. H., Nahm, S., Paik, J. H., Whang, K. C. and Ahn, B. G., Crystal structure and microwave dielectric properties of La $(Mg_{1/2}Ti_{1/2})O_3$ ceramics. *J. Mater. Sci. Lett.*, 2000, **19**, 131–134.
5. Cho, S. Y., Youn, H. J., Lee, H. J. and Hong, K. S., Contribution of structure to temperature dependence of resonant frequency in the $(1-x)La(Zn_{1/2}Ti_{1/2})O_3$–$xATiO_3$ (A = Ca, Sr) system. *J. Am. Ceram. Soc.*, 2001, **84**(4), 753–758.
6. Cho, S. Y., Kim, I. T. and Hong, K. S., Crystal structure and microwave dielectric properties of $(1-x)La(Zn_{1/2}Ti_{1/2})O_3$–$xATiO_3$ System. *Jpn. J. Appl. Phys.*, 1998, **37**(2), 593–596.
7. Kucheiko, S., Kim, H. J., Yeo, D. H. and Jung, H. J., Microwave dielectric properties of $LaZn_{0.5}Ti_{0.5}O_3$ ceramics prepared by sol-gel process. *Jpn. J. Appl. Phys.*, 1996, **35**(2A), 668–672.
8. Ferreira, V. M. and Baptista, J. L., Preparation and microwave dielectric properties of pure and doped magnesium titanate ceramics. *Mat. Res. Bull.*, 1994, **29**(10), 1017–1023.
9. Davies, P. K., Tong, J. and Negas, T., Effect of ordering-induced domain boundaries on low-loss $Ba(Zn_{1/3}Ta_{2/3})O_3$–$BaZrO_3$ perovskite microwave dielectrics. *J. Am. Ceram. Soc.*, 1997, **80**(7), 1727–1740.
10. Kim, I. T., Kim, Y. H. and Chung, S. J., Order-disorder transition and microwave dielectric properties of $Ba(Ni_{1/3}Nb_{2/3})O_3$ ceramics. *Jpn. J. Appl. Phys.*, 1995, **34**(1), 8 A 4096-4103.
11. Colla, E. L., Reaney, I. M. and Setter, N., Effect of structural changes in complex perovskites on the temperature coefficient of the relative permittivity. *J. Appl. Phys.*, 1993, **74**(5), 3414–3425.
12. Kim, J. S., Lee, J. H., Lim, Y. S., Jang, J. W. and Kim, I. T., Revisit to the anomaly in dielectric properties of $(Ba_{1-x}Sr_x)(Zn_{1/3}Nb_{2/3})O_3$ solid solution system. *Jpn. J. Appl. Phys.*, 1997, **36**(1), 5558–5561 9A.
13. Seabra, M. P. and Ferreira, V. M., Synthesis of $La(Mg_{0.5}Ti_{0.5})O_3$ ceramics for microwave applications. *Mat. Res. Bull.*, 2002, **37**, 255–262.
14. Avdeev, M., Seabra, M. P. and Ferreira, V. M., Crystal structure of dielectric ceramics in the $La(Mg_{0.5}Ti_{0.5})O_3$–$BaTiO_3$ system. *J. Mat. Res.*, 2002, **15**(5), 1112–1117.
15. Levin, I., Chan, J. Y., Maslar, J. E., Vanderah, T. A. and Bell, S. M., Phase transitions and microwave dielectric properties in the perovskite-like $Ca(Al_{0.5}Nb_{0.5})O_3$–$CaTiO_3$ system. *J. Appl. Phys.*, 2001, **90**(2), 904–914.
16. Meden, A. and Ceh, M., Rietveld refinement of $Ca_{0.54}La_{0.46}Mg_{0.23}Ti_{0.77}O_3$—a promising new microwave ceramic. *Materials Science Forum*, 2000, **231–234**, 988–993.
17. Avdeev, M., Seabra, M. P. and Ferreira, V. M., Structure evolution in $La(Mg_{0.5}Ti_{0.5})O_3$–$SrTiO_3$ system. *Mat. Res. Bull.*, 2002, **37**(8), 1459–1468.
18. Larson, A.C. & Von Dreele, R.B., Los Alamos National Laboratory Report No LAUR-86-748 (1987).
19. Hakki, B. W. and Coleman, P. D., *IRE Trans Mic Theory and Tech.*, 1960, **8**, 402–410.
20. Kajfez, D. and Guillion, P., *Dielectric Resonators*. Artech House, Zurich, Switzerland, 1986.
21. Matsumoto, H., Tamura, H. and Wakino, K., $Ba(Mg,Ta)O_3$–$BaSnO_3$ high-Q dielectric resonator. *Jpn. J. Appl. Phys.*, 1991, **30**, 2347–2349.
22. Kingery, W. D., *Introduction to Ceramics*. John Wiley & Sons, New York, 1976.
23. Kucheiko, S., Choi, J. W., Kim, H. J. and Jung, H. J., Microwave dielectric-properties of $CaTiO_3$–$Ca(Al_{1/2}Ta_{1/2})O_3$ ceramics. *J. Am. Ceram. Soc.*, 1996, **79**(10), 2739–2743.
24. Santha, N., Jawahar, I. N., Mohanan, P. and Sebastian, M. T., Microwave dielectric properties of $(1-x)CaTiO_3-xSm(Mg_{1/2}Ti_{1/2})O_3(0.1 \geqslant x \geqslant 1)$ ceramics. *Mat. Lett.*, 2002, **54**(4), 318–322.
25. Penn, S. J., Alford, N.McN., Templeton, A., Wang, X., Xu, M., Reece, M. and Schrapel, K., Effect of porosity and grain size on the microwave dielectric properties of sintered alumina. *J. Am. Ceram. Soc.*, 1997, **80**(7), 1885–1888.